Phys Chem Minerals (1984) 11:204–212

PHYSICS AND CHEMISTRY OF MINERALS

Hydrogen Speciation in Synthetic Quartz

Roger D. Aines[1] *, Stephen H. Kirby[2], and George R. Rossman[1]

[1] California Institute of Technology, Div. Geological and Planetary Sciences, Pasadena, California 91125, USA
[2] U.S. Geological Survey, 345 Middlefield Road, Menlo Park, California 94025, USA

Abstract. The dominant hydrogen impurity in synthetic quartz is molecular H_2O. H–OH groups also occur, but there is no direct evidence for the hydrolysis of Si–O–Si bonds to yield Si–OH HO–Si groups. Molecular H_2O concentrations in the synthetic quartz crystals studied range from less than 10 to 3,300 ppm (H/Si), and decrease smoothly by up to an order of magnitude with distance away from the seed. OH^- concentrations range from 96 to 715 ppm, and rise smoothly with distance away from the seed by up to a factor of three. The observed OH^- is probably all associated with cationic impurities, as in natural quartz. Molecular H_2O is the dominant initial hydrogen impurity in weak quartz. The hydrolytic weakening of quartz may be caused by the transformation $H_2O + Si-O-Si \rightarrow 2SiOH$, but this may be a transitory change with the SiOH groups recombining to form H_2O, and the average SiOH concentration remaining very low. Synthetic quartz is strengthened when the H_2O is accumulated into fluid inclusions and cannot react with the quartz framework.

Table 1. Indexing of synthetic quartz peaks in the near infrared region

Peak location		Species	Vibration
nm	cm^{-1}		
1,420	7,000	Both H_2O and OH^-	First overtone of stretching motions, ($\sim$3,500 cm^{-1})
1,920	5,200	H_2O	Stretch ($\sim$3,500 cm^{-1}) + bend (1,650 cm^{-1})
2,250	4,500	XOH, (X+H)	Stretch ($\sim$3,500 cm^{-1}) + bend (e.g., Al–O–H at $\sim$950 cm^{-1})
2,500	4,000	Both H_2O and OH^-	Stretch ($\sim$3,500 cm^{-1}) + an unspecified lattice mode at $\sim$500 cm^{-1}

Introduction

Synthetic quartz frequently contains hydrogen as a trace impurity (Kats 1962; Dodd and Fraser 1965, 1967; Kirby 1984). It is known to affect the mechanical properties by causing crystals with high hydrogen contents to deform plastically at low stress, while anhydrous crystals are strong and brittle (Griggs and Blacic 1965). The yield strength of synthetic crystals decreases with increasing total hydrogen concentration (Kirby and McCormick 1979).

The way that hydrogen is incorporated into synthetic quartz has been the subject of much discussion (e.g. Kirby 1984; Kekulawala et al. 1981). However, the appropriate diagnostic measurements necessary to determine the speciation have not been made. We have undertaken a study of hydrogen speciation using near infrared spectroscopy. By observing the spectrum of hydrogen species in this region we are able to quantitatively differentiate between hydrogen as OH^- groups and molecular H_2O. This method is described and reviewed by Aines and Rossman (1984a), and has been used to determine the speciation of hydrogen in opal (Langer and Flörke 1974), chalcedony (Flörke et al. 1982), and in silicate glasses (e.g. Scholze 1960; Stone and Walrafren 1982; Bartholomew et al. 1980). Details of peak assignments are given in these papers. We have briefly summarized them, as applied to quartz, in Table 1.

We have studied a suite of synthetic quartz crystals in detail, looking at hydrogen speciation and its relationship to hydrogen zonation. In addition, we have studied a number of natural and synthetic SiO_2 phases in order to obtain an understanding of the actual sites that hydrogen occupies in synthetic quartz. Opal (Langer and Flörke 1974) contains hydrogen in three forms: liquid water, isolated water, and hydroxide. Chalcedony (Flörke et al. 1982; Frondel 1982) contains hydroxide and water interpreted to occupy interstices at high angle grain boundaries and on the surfaces of fibers. Milky quartz contains hydrogen primarily as H_2O in fluid inclusions (e.g. Aines and Rossman 1984a).

A silica glass containing 8 percent H_2O was also studied. This glass is of particular interest because of its high water content, and the known hydrolysis of Si–O–Si bonds in glasses by water. In pure SiO_2 glasses, OH^- groups can be formed by hydrolysis of a Si–O–Si bond to make Si–OH HO–Si (Stone and Walrafren 1982). Similar hydrolysis mechanisms form the basis of most theories of hydrolytic weakening of quartz, and simple hydrolysis was the original

* Current Address: Lawrence Livermore National Laboratory, Earth Science Division, P.O. Box 808, Livermore, CA 94550, USA

Table 2. Growth histories and trace element analyses of Bell Laboratories synthetic quartz crystals

Crystal No.	Solvent	Tg, °C	ΔT, °C[a]	Fluid pressure, MPa	Growth rate[b] mm/day	Na[c]	K[c]	Li[d]	Al[d]	Fe[d]	Spectrum No.[e]
X-0	Conditions not known					300 (582)	8 (10)	21 (182)	56 (125)	33 (35)	1, 2
X-13	0.5 M NaOH 0.75 M KOH + Fe doping	342	52	177	2.20	160 (310)	196 (251)	<2 <17	60 (134)	76 (81)	1
X-41	1.0 M NaOH + BeO	350	56	–	2.16	100 (194)	<40 (<51)	<2 (<17)	54 (120)	<3 (<3)	
X-43	1.0 M NaOH + TiO_2	346	56	–	2.11						
X-116	Conditions not known										
X-246-23	1.0 M NaOH 0.1 M $LiCO_3$ 0.1 M $NaNO_3$	358	38	172	0.99						
X487	1.0 M NaOH 0.025 M $LiCO_3$ 0.1 M $NaNO_3$	339	58	291	2.66						
X488	1.0 M NaOH	377	22	152	1.57						
X-507-15 (near seed)	1.0 M NaOH	338	33	138	1.60	126 (244)	24 (27)	<2 (<17)	<30 (<67)	<3 (<3)	1, 5
X-507-15 (near outer surface)						26 (50)	<5 (<16)	<2 (<17)	<30 (<67)	<3 (<3)	2, 4

[a] Temperature difference between hotter nutrient chamber and growth chamber (see Laudise, 1959, 1973 for details on growth technique)
[b] Expressed as increase in crystal thickness in direction normal to growth direction (5° from [0001]). Twice average velocity of growth interface
[c] Determined by flame photometry, units ppm weight oxide/weight SiO_2 (ppm cation/Si). Analyst: Paul Klock, U.S.G.S., Menlo Park
[d] Determined by emission spectroscopy, units ppm weight element/weight SiO_2. Analyst: Terry Fries, U.S.G.S., Menlo Park
[e] Chemical analysis corresponds to region irradiated in the spectrum numbers indicated in Table 3

mechanism of hydrolytic weakening proposed by Griggs and Blacic (1965). They suggested that centers of hydrolysis could be mobile and localized at dislocations. Freiman (1984) summarizes work on crack growth in which similar mechanisms participate. The spectra of hydrous silica glass provides the best spectroscopic evidence for this type of hydrolysis. We have used the evidence from these model systems to infer the actual sites for hydrogen in synthetic quartz.

Hydrogen concentrations in synthetic quartz have been previously determined by bulk analytical techniques. We have correlated these measurements with our spectroscopic measurements to arrive at molar absorption coefficients which enable us to determine absolute concentrations of H_2O and OH^-.

Experimental

Samples

Synthetic quartz samples used in this study were grown at Bell Laboratories. Details of the growth history are given in Table 2. The crystals were cut so that they could be observed spectroscopically with the beam path parallel to the seed plate. This was done so that zonation away from the seed could be studied. Six of the crystals were cut as *ac* sections so that dichroism could be studied; X-488-3

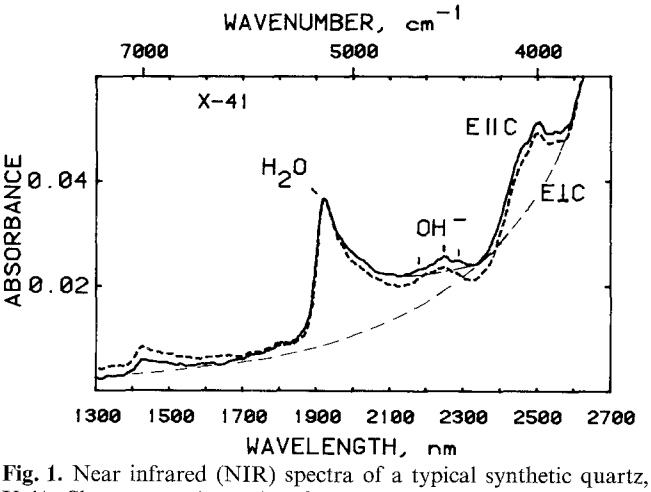

Fig. 1. Near infrared (NIR) spectra of a typical synthetic quartz, X-41. Shown are absorption features due to molecular H_2O at 1,920 nm, multiple peaks centered at 2,250 nm due to X-OH-groups, (X+H), and two bands due to both H_2O and X-OH at 1,410 and 2,500 nm. These are superimposed upon a strong background absorption due to O–H stretch at 2,900 nm (3,400 cm^{-1}). Spectra are taken with light polarized $E \| c$ (ω), solid trace, and $E \perp c$ (ε), dotted trace, with the beam path parallel to the seed plate. Sample thickness 2.44 cm, spectra taken with 2.0 mm aperture placed 3.4 mm from the seed. Crystal contains ~900 ppm H/Si, predominately as H_2O. Also shown (long dashes) are baselines used to determine individual peak heights

Table 3. Synthetic quartz absorbances and calculated hydrogen concentrations

Sample	Spectra[a], polarization	ppm H/Si[b]	Distance[c] from seed (mm)	Peak intensities Abs/cm[d]				Hydrogen concentration by species (ppm H/Si)[e]					
				1,420 nm (Total H)	1,920 nm (H_2O)	2,250 nm (OH^-)	2,500 nm (Total H)	H_2O (1,920 nm)		OH^- (2,250 nm)		Total H	
								$\varepsilon=0.5$	$\varepsilon=0.6$[f]	$\varepsilon=0.4$	$\varepsilon=0.8$[g]	upper	lower[h]
X-0	#1 $E\|\|c$	3,310	13	0.00534	0.04209	0.00276	0.02100	3,817	3,181	313	156	4,130	3,337
	#2 $E\|\|c$	2,912	11	0.00406	0.03329	0.00295	0.01752	3,020	2,516	334	167	3,354	2,683
X-13	#1 $E\|\|c$(basal)	1,770	13	0.00316	0.02461	0.00631	0.01974	2,232	1,860	715	358	2,950	2,218
	#2 $E\|\|c$(fast a)[j]			0.00309	0.02316	0.00382	0.01684	2,100	1,750	388	194	2,488	1,944
X-41	#1 $E\|\|c$	846	3.42	0.00109	0.01018	0.00144	0.00675	1,000	832	163	81	1,163	913
	#2 $E\|\|c$		1.48	0.00123	0.01008	0.00079	0.00520	914	762	90	45	1,004	807
	#3 $E\|\|c$		6.98	0.00118	0.01005	0.00115	0.00682	912	760	130	65	1,042	825
X-43	#1 $E\|\|c$	860	17.5	0.00105	0.1024	0.00315	0.00737	929	774	357	179	1,286	953
X-116	#1 $E\|\|c$	1,112	6,54	0.00184	0.01414	0.00250	0.00895	1,282	1,069	283	142	1,565	1,211
	#2 $E\|\|c$		2.20	0.00221	0.02005	0.00174	0.01579	1,818	1,515	197	98	2,015	1,693
	#3 $E\|\|c$		11.08	0.00112	0.00618	0.00484	0.00655	560	467	549	274	1,109	741
	#4						(no data)						
	#5 $E\|\|c$		8.72	0.00112	0.01125	0.00335	0.00734	1,020	850	380	190	1,400	1,040
	#6 $E\|\|c$		9.06	0.00138	0.01016	0.00312	0.00766	921	768	354	176	1,275	935
X-487-2	#1 $E\|\|c$		1.98	0.00221	0.01697	0.00138	0.01247	1,540	1,282	156	78	1,696	1,360
	#2 $E\|\|c$	531	8.34	0.00079	0.00455	0.00198	0.00411	413	344	225	112	638	456
X-488-3	#1 $E\perp c$	42	3.58	–[i]	–[i]	0.00085	0.00145	–	–	96	48	96	48
Rhomb. growth	#2 $E\perp c$		1.28	–	0.00015	0.00067	0.00134	14	11	76	38	90	49
X-507-15(2)	#1 $E\|\|c$		5.00	0.00095	0.00732	0.00163	0.00568	664	553	185	92	849	645
	#2 $E\|\|c$	305	12.62	0.00043	0.00364	0.00184	0.00306	330	275	208	104	538	379
	#3 $E\|\|c$	156	20.90	0.00030	0.00053	0.00391	0.00570	48	40	443	221	491	261
	#4 $E\|\|c$		16.64	0.00042	0.00229	0.00283	0.00384	208	173	321	160	529	333
	#5 $E\|\|c$	396	1.84	0.00134	0.00809	0.00137	0.00762	734	611	155	78	889	689

[a] All are $E\|\|c$ except X-488-3, which did not have that polarization available

[b] Estimates obtained from integrated intensity in the 3,400 cm^{-1} region (Kirby 1984)

[c] Distance to center of 2.0 mm round aperture along perpendicular line from seed. All spectra measured with the beam path parallel to the seed

[d] Measured, using estimated baseline. Baseline was constrained to be the same as the spectra at 1,350, 1,700, and 2,600 nm. Baseline for 2,250 peaks takes into consideration significant contribution from the 1,920 peak. Estimated measurement errors: 1,420 nm ± 15 percent, 1,920 nm ± 4 percent, 2,250 nm ± 10 percent, 2,500 nm ± 15 percent

[e] ppm $H/Si=[A(cm^{-1})/\varepsilon(mol\cdot l^{-1}\,cm^{-1})]\cdot 2\cdot 10^6/[SiO_2\,mol\cdot l^{-1}]=(A/\varepsilon)\cdot 45{,}350$. A=absorbance, ε=molar extinction coefficient from Beer's Law in terms of H_2O, factor of 2 converts to OH, 10^6 converts to ppm, and concentration of SiO_2 per liter converts the H concentration from moles/liter to moles/mole of SiO_2

[f] H_2O ε values constrained to reproduce the known range for X-0, ~4,000–3,000 ppm. Since H_2O dominates most of the samples, this should accurately measure total H. The indicated ε values bracket the total H concentrations well except for samples X-43 (too low) and X-487-2 (too high)

[g] OH^- ε values constrained to bracket X-488-3 total H concentrations. This crystal was measured with $E\perp c$, unlike the others. $E\|\|c$ yields less intense OH^- spectra, so the ε values for $E\perp c$ may in fact be higher

[h] Calculated by adding the H_2O and OH^- contents from NIR measurements. Some of the differences between this measurement and the IR measurements (note 2) may be attributed to slightly differing paths in the thick NIR samples. This is particularly noticeable very close to the seed, e.g., X-507 point # 5

[i] No absorption bands detected

[j] This sector is light blue with growth in fast a direction. Fe doped 80 ppm

and X-43 were not. For near infrared work all samples were 2 to 5 cm thick, which is required to obtain suitably intense spectra. For infrared work (used for calibrating the concentrations) samples were 0.1 to 0.3 cm thick.

Natural samples used in this study were chosen as typical examples of the major silica minerals that can serve as model systems for synthetic quartz. They are: 1) opal, from Opal Mt., San Bernardino County, California, CIT # 13027, 2) chalcedony from a geode wall lining, Chihuahua, Mexico (Finkelman et al. 1974), CIT # 10100, and 3) milky quartz, Dillsburg, Pennsylvania, CIT # 3032. In addition to these natural samples, a SiO_2 synthetic glass was used which contains approximately 8 percent H_2O, prepared in a piston cylinder apparatus at 12 Kbar, 1400° C by A. Boettcher, UCLA, his # 2568.

Spectroscopy

Near infrared (NIR) spectra were obtained using a Cary 17I spectrophotometer, and infrared (IR) spectra were ob-

tained using a Perkin Elmer 180 spectrophotometer, with techniques described by Goldman et al. (1977). Measurements used for concentration determinations were made at room temperature. Additional measurements were made at −196° C. NIR spectra were then digitally encoded and corrected for the spectrometer baseline. Peak height data were obtained by applying a smooth baseline, constrained to coincide with the spectrum at 1,350, 1,700, and 2,600 nm, where there are no hydrogen-related absorptions. A typical baseline is shown in Figure 1. In H_2O-rich samples, a correction was made for the overlap of the 1,900 nm H_2O band and the 2,250 nm OH^- (also shown in Fig. 1). It was not possible to apply a nonarbitrary baseline to these spectra because the broad features that underlie the peaks of interest are themselves functions of the hydrogen content of the crystal. The principal contribution to these broad underlying absorptions comes from O−H stretch fundamentals in the 3,000 nm (3,500 cm^{-1}) region which are very intense at the thicknesses for NIR studies. Therefore, an *a priori* baseline cannot be applied. The inherent inaccuracy of applying an arbitrary baseline is the primary error in the measurement, discussed in Table 3. Integral absorption in the near-infrared region was not measured because of overlapping peaks. However, data from Kirby (1984) indicate that peak and integral absorption may be used interchangeably for the IR region of quartz, and Stolper (1982) has shown that for H_2O and OH^- in silicate glasses, peak and integral absorption are interchangeable in the NIR region.

Infrared spectra were obtained at the identical locations used for NIR spectra. After the NIR spectra were run, the samples were cut to appropriate thicknesses for IR work. The IR spectra were corrected for intrinsic SiO_2 absorption modes using the spectrum of a very dry synthetic quartz, X-246-3 which contains ~40 ppm H/Si. Spectra were polarized, with $\mathbf{E} \perp C$. These spectra were used to calculate the total H_2O content of the crystals at the locations measured (Kirby 1984). The reference sample of X-0 used by Kirby was also measured, and a six-point zoning profile was measured in order to obtain an accurate average value for this slab. This yielded a calibration factor (for these techniques and instruments) of

$$\text{Concentration H/Si (ppm)} = 1.05 \times A\,(\text{cm}^{-2})$$

where A = integral absorbance from 3,750 cm^{-1} to 2,400 cm^{-1}, suitably corrected for background Si−O absorptions.

Results

Hydrogen Speciation

Synthetic quartz contains trace hydrogen both as molecular H_2O and OH^- groups. As the hydrogen content of the crystal increases, so does the H_2O content. Samples that are weak and ductile, such as X-0 (Griggs and Blacic 1965), contain molecular water as the dominant hydrogen-containing species.

Figure 1 shows a typical spectrum of synthetic quartz in the near infrared region. This crystal contains approximately 900 ppm H/Si. The individual absorptions due to both molecular H_2O and OH^- groups in this crystal are identified. The broad, sloping shoulder (rising at long wavelengths) upon which these peaks are superimposed is due

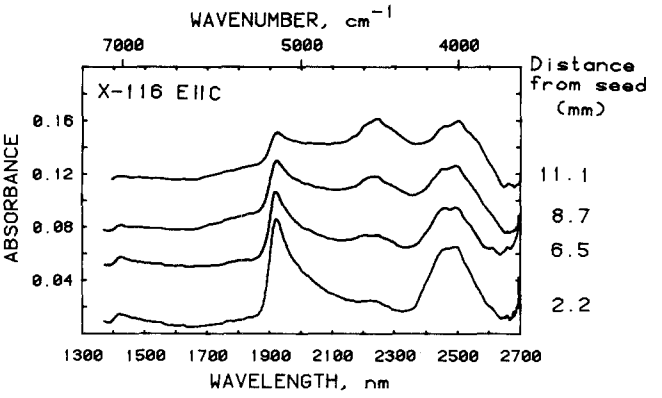

Fig. 2. NIR spectra of synthetic quartz X-116 showing changes in the absorption features as a function of distance away from the seed plate: H_2O (1,920 nm) decreases and OH^- (2,250 nm) increases. Spectra have had the strong background absorption seen in Fig. 1 removed. Sample thickness 3.79 cm, light polarized $E \| c$

to the intense O−H stretching fundamental at 3,400 cm^{-1}. Some spectral features are slightly anisotropic. The underlying absorption changes depending on the polarization of the spectrum. There are also changes in the OH^- band at 2,250 nm. In the $\mathbf{E} \| c$ spectrum the band is dominated by a peak at 2,250 nm, and in the $\mathbf{E} \perp c$ spectrum there are three approximately equal peaks. The overall intensities are similar in both polarizations. This polarization of the OH^- band is typical of the synthetic quartzes studied. Contrasting with this is the lack of polarization of the band due to molecular H_2O at 1,920 nm. The apparent differences in shape seen in Fig. 1 for this band are attributable to polarized contributions from sharp band absorptions in the 3,500 cm^{-1} region. When the H_2O band is present, it is always essentially isotropic.

The crystals we studied are strongly zoned in H_2O, OH^-, and total hydrogen content. Figure 2 shows the spectra of crystal X-116 at various distances from the seed. (These spectra have had the broad background absorption due to intense bands in the 3,500–3,000 cm^{-1} region removed by subtraction of a scaled, computer fitted baseline similar to that seen in Fig. 1. The same baseline was used for all the spectra with the scaling factor varied to bring the absorbance at 2,650 nm to the same level as at 1,650 nm. This apparently results in too great an intensity in the 2,200 nm region for low hydrogen samples.) Near the seed, the crystal is dominated by H_2O, which decreases away from the seed while OH^- rises in concentration.

Table 3 summarizes the results of our near infrared studies of synthetic quartz. Using hydrogen contents determined from the integral absorbance in the 3,500 cm^{-1} region (Kirby 1984), we have calculated peak height molar absorption coefficients (ε) for hydrogen (as H_2O). It is conventional (Bartholomew et al. 1980) to report both OH^- and H_2O ε values as H_2O since that is the species measured by other techniques such as weight loss measurements. For hydroxide, there are actually twice as many moles (OH^-)/liter than would be calculated from the ε value. In Table 3 we show two ε values for each species, representing the range of values which fit the previously determined total hydrogen concentrations. The $\varepsilon(OH^-)$ values are not as well constrained because of the low OH^- content of all the crystals. The best fit appears to be with ε values for both H_2O and OH^- of ~0.5 (l $\text{mole}_{H_2O}^{-1}$ cm^{-1}).

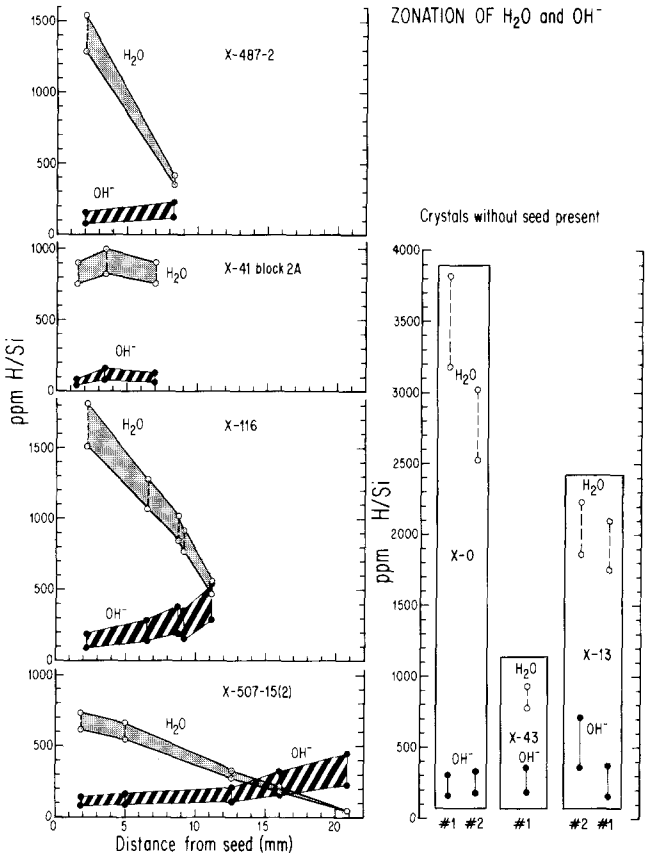

Fig. 3. Concentration of OH^- and H_2O as a function of distance from the seed plate. Ranges shown are from the ε values calculated to bracket the known total hydrogen content of the samples (Table 3). Also shown are OH^- and H_2O concentrations for three samples for which the seed location is not known; numbers refer to the spectra numbers in Table 3

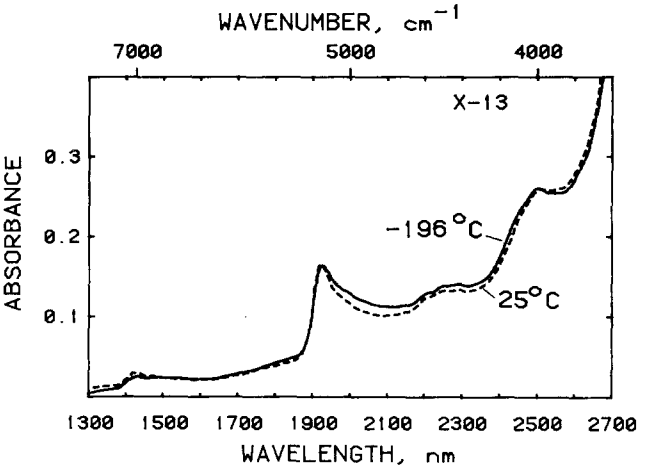

Fig. 4. Temperature dependence of the NIR absorption features. No new band forms at 2,000 nm, showing that there is no liquid water that can convert to ice when cooled. Quartz X-13, basal growth zone, 4.7 cm thick. Light polarized $E \| c$

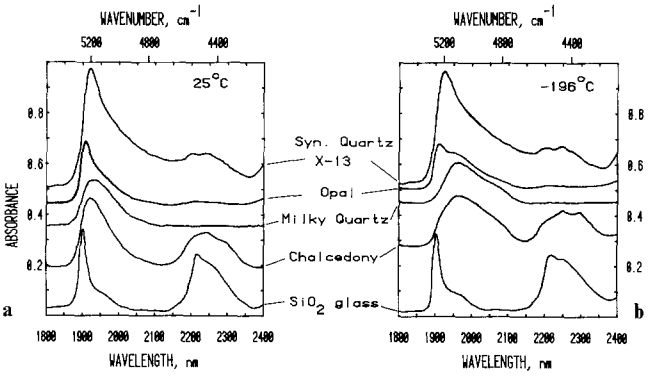

Fig. 5a and b. Comparison of the NIR absorptions due to H_2O ($\sim$1,920 nm) and OH^- ($\sim$2,250 nm) in SiO_2. **a)** 25° C, **b)** −196° C. All spectra taken with unpolarized light. SiO_2 glass, Boettcher # 2568 0.045 cm thick; chalcedony, Chihuahua, Mexico 0.46 cm; milky quartz, Dillsburg, Pennsylvania 0.033 cm; opal, San Bernardino County, California 0.039 cm; and synthetic quartz X-13 basal growth zone (seen in Fig. 5) plotted here as 19 cm thick. The offsets of the baselines from 25° C to −196° C are arbitrary. Spectra have had background absorption removed as in Fig. 2

The range of molecular H_2O contents is from 0 ppm (X-488-3) to 3,300 ppm H/Si (X-0). The range of OH^- concentrations is from 96 (X-488-3) to 715 ppm H/Si (X-13, basal growth). Figure 3 summarizes the zoning profiles in terms of concentration and distance from the seed (all for basal (0001) growth samples). The seed was not contained in our samples of X-0, X-43, and X-13, but we were able to determine the approximate distance from the seed from records kept during cutting of the original samples. Two common trends emerge from Fig. 3: the H_2O concentration decreases dramatically and the OH^- concentration rises gradually with greater distance from the seed. The ranges shown here are calculated from the two ε values for each species shown in Table 3. Even if these values were known to greater accuracy, the concentration slopes would remain sub-parallel to the trends shown. The H_2O/OH ratios are independent of the absolute hydrogen concentration. The estimated error in measurement of individual absorbance values is about 10%. This error is random, unlike the systematic error introduced by uncertainty in the ε values. Within error, then, we can confidently say that H_2O decreases and OH^- increases in all samples but X-41, in which both remain constant within error.

H_2O and OH^- Sites; Comparison with Other SiO_2 Systems

H_2O. The major hydrogen impurity in synthetic quartz is H_2O. In order to determine whether the H_2O molecules occur individually, in groups, or as fluid inclusions, we have studied the spectra at −196° C. This method allows us to distinguish fluid inclusions containing enough water molecules to freeze to ice, as evidenced by an ice band in the spectrum at 2,000 nm (Dodd and Fraser 1967; Aines and Rossman 1984a). X-0 and X-13 were studied by this method. Ice bands were not observed. Figure 4 shows that there is very little difference between the 25° C and −196° C spectrum, the major difference being a broadening of the 1,920 nm peak toward long wavelengths.

Figure 5a and b show the freezing behavior of the other SiO_2 compounds as well as that of X-13 for comparison. They have been stacked to compare peak locations and shapes. The H_2O region in silica glass contains two components, the sharper one peaking at 1,905 nm. It does not change when the sample is frozen. Chalcedony and milky quartz have broad H_2O peaks that shift substantially when frozen, as is expected for liquid water. In opal an ice band forms at 1,980 nm, but the original 25° C peak at 1,910 nm remains as well, indicating two water types as suggested

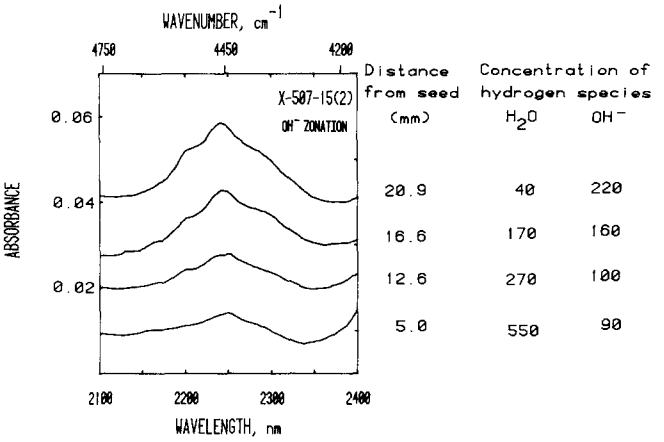

Fig. 6. Expanded view of the X-OH region in the NIR at 2,250 nm, showing the change in the OH pattern with distance from seed and the molecular H_2O concentration for crystal X-507. There is no correlation between H_2O concentration and the shape of the OH^- peaks or their intensity, indicating no equilibrium relationship between the concentrations of H_2O and OH^-. Crystal 4.75 cm thick, light polarized $E \| c$. Spectra have had background absorption removed as in Fig. 2

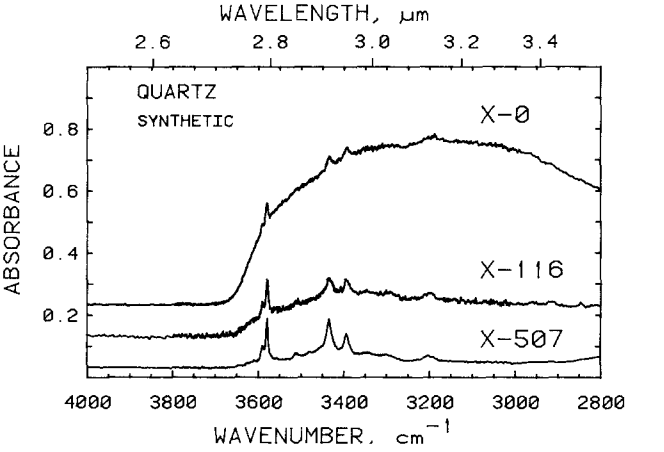

Fig. 7. IR spectra as three of the samples measured in the NIR. Spectra recorded at −196° C, plotted normalized to 1 mm thickness, and offset vertically for clarity

by Langer and Flörke (1974). However, none of these system's behavior is identical to synthetic quartz.

OH^-. Comparison of the temperature effect on the hydroxide regions in Fig. 5 shows that there are no major changes. In SiO_2 glass the hydroxide peaks are located at 2,220 and 2,250 nm. The pattern is markedly different from synthetic quartz. Chalcedony has a broad band in the 2,250 region that is similar to synthetic quartz, but has less spectral structure apparent. The opal pattern is similar when expanded vertically (not illustrated).

The change in the OH^- spectrum with distance from the seed is shown in Fig. 6 for crystal X-507. Despite a change in OH^- concentration from 90 to 200 ppm, there appears to be no change in the shape of the band. This is true for other samples as well, although from sample to sample there are minor differences. Most importantly, none of the peaks in this region have any correlation with the H_2O content of the crystal.

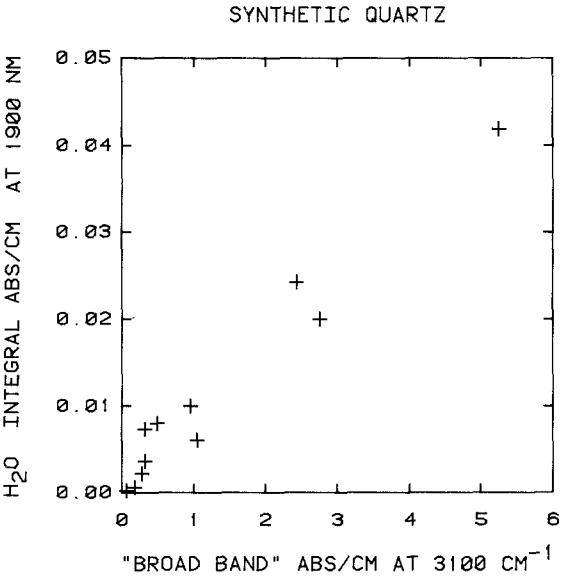

Fig. 8. Plot of absorbance of 1,900 nm (due to molecular H_2O) vs. broad band absorption, measured from the peak intensity at 3,100 cm^{-1}. Measurements made at 23° C. Spectra were also used to obtain total H_2O from the total integral absorbance in the 3,700–2,800 cm^{-1} region (Table 3)

Comparison of NIR and IR Spectra

Figure 7 shows IR spectra recorded at −196° C for three of the samples used in the NIR study. They range from very low H_2O (X-507) to high H_2O(X-0) contents. The broad band in the IR correlates with the 1,900 nm H_2O band in the NIR. Figure 8 shows the quantitative relationship between these two, where the IR broad band was measured by the absorption intensity at 3,100 cm^{-1}, where no sharp band absorption occurs. This was measured at 23° C from the runs used to measure water content from total integral IR absorption (Table 3). The general relationship between H_2O and broad band absorption is very good. The scatter in the graph (particularly noticeable for the X-507 points) appears to be due to inhomogeneity in the large crystals used for NIR measurements for the case of X-507. IR measurements were made on a 0.35 cm wafer cut from the original NIR sample which was more than 5 cm long. A more extensive study of the relationships between the NIR and IR absorptions will be required in order to obtain a more accurate graph than Fig. 8.

Discussion

The major hydrogen impurity in synthetic quartz is molecular H_2O. Hydroxide is always present but to a much smaller extent. The concentration of H_2O decreases away from the seed, and by inference decreases with growth rate (Kirby 1984). Hydroxide increases away from the seed. The major species responsible for initiating hydrolytic weakening in quartz appears to be H_2O, since it dominates the hydrogen speciation of weak quartz crystals and correlates with the broad band absorption previously identified in the IR region.

H_2O Site

Our NIR data show that the molecular H_2O in synthetic quartz is not in the form of fluid inclusions. Dodd and

Fraser (1965), Kirby and McCormick (1975), and Kekulawala et al. (1981) arrived at this conclusion based on the absence of an ice band in infrared studies at liquid nitrogen temperatures. In addition, Kirby and McCormick also made a TEM study of many of the same samples studied here which revealed no fluid inclusions, a result confirmed by Kekulawala et al. They did, however, find what they termed "features with the characteristics of sources of hydrostatic pressure." Even if these were very small fluid inclusions, though, careful counting of them reveals that they could only account for a small amount of the hydrogen in the crystal.

Our low temperature studies in the NIR region confirm that the H_2O in synthetic quartz is not in fluid inclusions. No ice band forms at 2,000 nm when the samples are frozen, and the room temperature peak shape is very different from that of liquid water such as that in the spectrum of milky quartz (Fig. 5a and b). The use of freezing to distinguish fluid inclusions is probably limited to groups of water molecules of a size resolvable by optical microscopy or TEM methods (Kekulawala et al. 1981). Groups approximately less than several hundred molecules cannot be distinguished in this way (Aines and Rossman 1984a). In order to understand the sites and groupings of very small groups or individual water molecules, it is instructive to look at the behavior of water in other silicas.

Individual water molecules trapped in voids in crystals or bonded into the structure tend to give sharp peaks and anisotropic behavior in the IR and NIR region (Aines and Rossman 1984a). This behavior is in sharp contrast to that of water in synthetic quartz. The water in synthetic quartz is not bonded into the structure in any coherent way because its spectrum is isotropic, in contrast to the behavior of trace water in cordierite (Goldman et al. 1977). This is in accord with the suggestion that the incorporation of water into quartz is not an equilibrium process (Kirby 1984). The water appears to be trapped by the rapidly growing quartz.

Langer and Flörke (1974) showed that opal contains water in two forms; type A, liquid water, and type B, water not strongly hydrogen bonded which they interpret as individual water molecules trapped in cages in the structure. At room temperature (Fig. 5a) the 1,900 nm region of opal is very similar to that of synthetic quartz. At low temperature type B water forms an ice band, in contrast to quartz. Figure 5b shows that the two opal water types are distinct at $-196°$ C, with the liquid (type A) forming an ice band at about 1,980 n, and the non-hydrogen bonded water molecules (type B) remaining very similar to the room temperature spectrum. Thus, it appears that the water in synthetic quartz, which behaves very similarly upon freezing, may be related to the individual water molecules (type B) in opal. In chalcedony Flörke et al. (1982) conclude that the molecular water present is all of type B, in analogy to opal. This is in accord with Frondel's (1982) IR study of chalcedony which showed a consistent broad band at 3,400 cm^{-1}. This is the characteristic signature in the IR region of liquid water. Our freezing study of chalcedony showed that the typical ice band forms (Fig. 5b) but in contrast to liquid water in fluid inclusions, chalcedony maintains a distinct shoulder at 1,930 nm when frozen. This is similar to opal and suggests that there are two water types in chalcedony as well. Chalcedony is completely dominated by liquid water, however, in contrast to synthetic quartz.

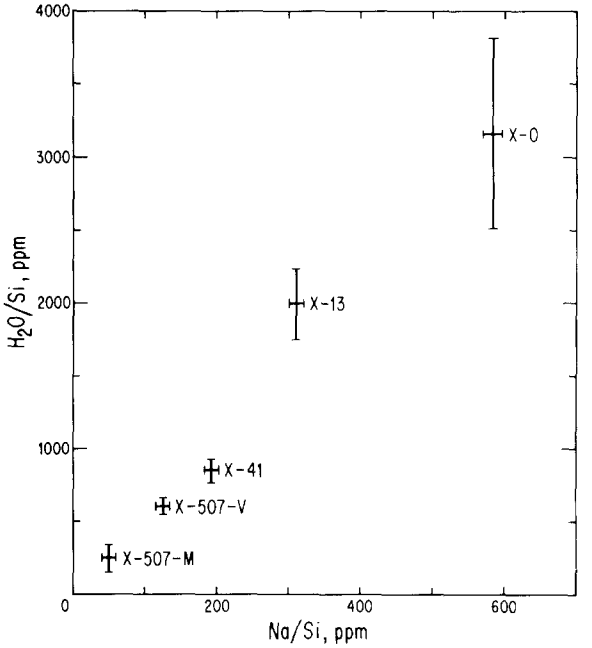

Fig. 9. Correlation between H_2O in molecular form and Na content, both expressed as atomic ratio to silicon. There are approximately five H_2O molecules for every Na atom

Of all the systems studied, the 1,905 nm band of SiO_2 glass occurs at the shortest wavelength. Like opal (type A) and quartz, this band does not shift when frozen. An additional smaller band is seen at 1,970 nm, which also does not shift. These may be due to individual water molecules (1,905 nm) and some form of hydrogen bonded water molecules, possibly in small clusters (1,970 nm). The difference in the H_2O absorption wavelength between SiO_2 glass and H_2O in crystalline SiO_2 is significant. The water in quartz is probably in larger groups than in the glass, or it is hydrogen bonded to hydroxyl groups. In either situation, hydrogen bonds would shift the absorption to longer wavelengths.

There is a definite correlation between H_2O and Na^+ content of the synthetic quartz studied here. Figure 9 shows that there are about five water molecules for every Na^+ atom. There is no correlation between Na^+ and OH^- (compare Figs. 3 and 7), which appears to severely limit the possible concentration of species such as NaOH, because Na and OH exist at similar concentrations in these samples. It is possible that water and Na^+ actually exist in units of this stoichiometry within the crystals, perhaps as a result of the occlusion of hydrated Na^+ ions. However, H_2O and Na^+ may simply have effective kinetic fractionation coefficients (during occlusion by rapid crystal growth) that differ by 5:1, resulting in this ratio within the crystal but with no genetic relationship between the two impurities.

The hydrogarnet substitution, $H_4O_4^{4-} \rightleftarrows SiO_4^{4-}$, has been proposed as the hydrogen speciation in mechanically weak quartz (McLaren et al. 1983; Nuttal and Weil 1980; Hobbs 1984). The presence of H_2O as the dominant hydrogen species rules out the possibility that the initial hydrogen defect is similar in form to the hydrogarnet substitution. Tetrahedral $(H_4O_4)^{4-}$ groups have only one hydrogen per oxygen, and would not give an absorption at 1,900 nm (Aines and Rossman 1984a). Adjacent "corner sharing" H_4O_4 tetrahedra could be "joined" by a water molecule,

but hydrogen speciation could still be dominantly hydroxide. There is no evidence of this in our NIR spectra, since H_2O is the predominant hydrogen species. Aines and Rossman (1984b) showed that garnets with up to four times more total H_2O (as H_4O_4) than quartz X-0 show no absorptions at 1,900 nm.

Water in quartz is not present as individual water molecules in distinct voids in the crystal structure, because it would give a sharper and anisotropic peak in the 1,900 nm region such as is found in the spectra of gypsum and cordierite (Aines and Rossman 1984a). It is also not present as liquid water (fluid inclusions) because an ice band does not form at low temperature. There are small changes in the 1,900 nm region of the low temperature spectrum, however; a definite increase in intensity around 1,950 nm occurs (Fig. 4). However, structure in the spectrum does not develop at low temperature and furthermore the peak position does not shift. The shape of the 1,920 nm band is distinctly different from that of individual water molecules, or liquid water; it is intermediate to these. We suggest that the water in synthetic quartz exists as small groups of water molecules which range in size. The lower limit of one molecule cannot be the dominant form because of the lack of anisotropy discussed above. An upper limit of approximately 200 molecules results from the lack of ice bands at low temperature (Kekulawala et al. 1981; Aines and Rossman 1984a). The size distribution appears to be skewed toward small clusters because of considerations relating peak wavelength so size of polymeric units of water (Van Thiel et al. 1957). The minor shifts in the 1900 nm region are due to incipient formation of ice in the larger groups, but the smaller groups undergo no change and the peak remains at 1,920 nm.

OH^- Site

The NIR spectroscopic properties of hydroxide in synthetic quartz are very similar to those of natural SiO_2 polymorphs. Hydroxide features occur in the 2,250 nm region in the NIR (Fig. 5) but are really best studied in the IR. The IR data have been discussed by Aines and Rossman (1984a) who concluded that many of the sharp peaks in synthetic quartz were identical to those resulting from hydrogen-alkali and hydrogen-aluminum defects in natural quartz. This association has not been made in the past because of the apparent lack of correlation between hydrogen content and the intensity of sharp bands in the IR region. This lack of correlation between total hydrogen and the *sharp* peaks is understandable, since in most synthetic quartz, molecular water is the major hydrogen species, and it yields the observed *broad* band spectrum in the IR 3,400 cm^{-1} region.

An important question is whether or not all of the hydroxide present in synthetic quartz is associated with cationic impurities or is in the form SiOH. The most plausible mechanisms of hydrolytic weakening involve the hydrolysis of Si–O–Si bonds, and formation of hydroxide in the form SiOH. The spectroscopic behavior of this species is known from SiO_2 glass (Stone and Walrafren 1982). Figure 5 shows that while SiO_2 glass and synthetic quartz both have absorptions in the 2,250 nm region, the glass is dominated by a peak at 2,210 nm and the overall patterns are different. The lack of similarity does not prove that some SiOH is not present. Figure 6 shows the hydroxide pattern of crystal X-507 obtained in regions of different H_2O contents. If H_2O were hydrolysing bonds to form SiOH, the concentration of SiOH should increase with the concentration of H_2O. If this happened, the bottom trace of Fig. 6 should have a more distinct SiOH pattern than the top in the 2,210 nm region. This does no happen; the hydroxide pattern in X-507 seems to remain constant in shape and only increases in concentration with distance away from the seed. The same OH^- defects occur throughout the crystal and are independent of H_2O concentration. There is no direct spectroscopic evidence for SiOH groups. Using the data for SiOH in glass, we estimate our limit of detection to be 5 ppm H/Si in the 2,210 nm region.

Conclusions

Hydrolytic Weakening

Kekulawala et al. (1981) have shown that quartz crystals that are intrinsically weak display a broad isotropic absorption band centered at about 3,400 cm^{-1}. Our spectroscopic work in the near infrared has proven that molecular water causes this characteristic "broad band" absorption. Griggs and Blacic (1965) and Griggs (1967) originally discovered the hydrolytic weakening phenomenon in dry natural quartz crystals that were annealed at high pressure in the presence of water and put forward the hypothesis that the following hydrolysis reaction is localized at crystal dislocations in quartz:

$$\equiv Si-O-Si\equiv \; + \; H_2O \rightleftarrows \equiv Si-OH : OH-Si\equiv \qquad (1)$$

where each dashed line represents a strong Si–O bond and the colon symbol represents the weak hydrogen bonds between silanol groups. If the reaction occurs at sites adjacent to dislocation cores, the activation barrier to dislocation motion would be reduced and dislocations as they move could shear the two silanol groups at low shear stresses. The silanol groups would therefore be short-lived transitional states and Si–OH groups at the "dangling" bonds at dislocation cores would exist metastably. Griggs (1974) showed that for typical dislocations densities that exist in quartz crystals, both as received and experimentally deformed, less than 1 ppm Si–OH/Si would saturate the dangling bonds at dislocations. Our isolation of molecular water as the mechanically-effective hydrogen species in synthetic quartz is completely consistent with the Griggs-Blacic hypothesis and lack of correlation of hydroxyl concentration with H_2O concentration (Table 3) indicates either that the equilibrium constant for Equation (1) is very low such that the expected hydroxyl concentration is below our level of detection or that the synthetic quartz is not in equilibrium according to the hydrolysis reaction. Stolper (1982) has shown that the reaction of Equation (1) applies to silicate glasses and that the equilibrium constant for the reaction $K = 0.2$. This is not surprising since glasses are not equilibrium phases and are thought to have many "dangling" bonds.

Speciation of Water in Low Temperature SiO_2 Polymorphs

Molecular water is an important constituent of quartz, opal, and chalcedony grown at low temperature. Synthetic and natural low temperature quartzes are identical spectroscopically (Aines and Rossman 1983) and the other polymorphs are similar. It seems likely that in all of these cases, molecular water is occluded during the growth of the crystals.

In chalcedony, the variety of fiber and grain sizes probably allows a continuous variation from individual water molecules to large fluid inclusions.

Opal contains two portions of the continuum of water environments found in chalcedony, one representing large aggregates of H_2O between the silica units, and another representing much smaller aggregates within the silica units themselves. The spectra of the internal water in opal, chalcedony, and low temperature crystalline quartz are very similar to the spectra of water in synthetic quartz. This suggests that all of these phases contain very small groups of water molecules which have a distribution in size. The major spectroscopic differences among these SiO_2 systems seem to arise from processes on the exterior and surface of grains, fibers, or crystallites.

Acknowledgements. Synthetic quartz was obtained from Bell Laboratories, Murray Hill, New Jersey, courtesy of David Fraser, Robert Laudise, and Ernie Kolb. Kurt Nassau (Bell Laboratories) provided helpful insight into the growth of synthetic quartz. Art Boettcher (UCLA) provided the hydrous SiO_2 glass and Ed Stolper (Caltech) provided its spectrum and water concentration. This work was supported in part by NSF Grant EAR 7919987 AO1.

References

Aines RD, Rossman GR (1984a) Water in minerals? A peak in the infrared. J Geophys Res 89:4059–4072

Aines RD, Rossman GR (1984b) The hydrous component in garnets. I. Pyralspites. Am Min (in press)

Bartholomew RF, Butler BL, Hoover HL, Wu CK (1980) Infrared spectra of a water containing glass. J Am Cer Soc 63:481–485

Dodd DM, Fraser DB (1965) The 3000–3900 cm^{-1} absorption bands and anelasticity in crystalline quartz. J Phys Chem Solids 26:673–686

Dodd DM, Fraser DB (1967) Infrared studies of the variation of H-bonded OH in synthetic alpha-quartz. Am Min 52:149–160

Finkelman RB, Evans HT Jr, Matzko JJ (1974) Manganese minerals in geodes from Chihuahua, Mexico. Min Mag 39:549–558

Flörke OW, Köhler-Herbertz B, Langer K, Tönges I (1982) Water in microcrystalline quartz of volcanic origin: agates. Contrib Mineral Petrol 80:324–333

Freiman SW (1984) Effects of chemical environments on slow crack growth in glasses and ceramics. J Geophys Res 89:4072–4076

Frondel C (1982) Structural hydroxyl in chalcedony (Type B quartz). Am Min 67:1248–1257

Goldman DS, Rossman GR, Dollase WA (1977) Channel constituents in cordierite. Am Min 62:1144–1157

Griggs DT (1974) A model of hydrolytic weakening in quartz. J Geophys Res 79:1653–1661

Griggs DT, Blacic JD (1965) Quartz: anomalous weakness of synthetic crystals. Science 147:292–295

Hobbs BE (1984) Point defect chemistry of minerals under a hydrothermal environment. J Geophys Res 89:4026–4038

Kats A (1962) Hydrogen in alpha-quartz. Philips Res Rep 17:133–279

Kekulawala KRSS, Paterson MS, Boland JW (1981) An experimental study of the role of water in quartz deformation. In: Carter NL et al. (eds) Mechanical Behavior of Crustal Rocks, The Handin Volume, Geophysical Monograph 24, American Geophysical Union, pp 49–60

Kirby SH, McCormick JW (1979) Creep of hydrolytically weakened synthetic quartz crystals oriented to promote $\{2\bar{1}\bar{1}0\}<0001>$ slip: a brief summary of work to date. Bull Miner 102:124–137

Kirby SH (1984) Hydrogen-bonded hydroxyl in synthetic quartz: analysis, mode of incorporation and role in hydrolytic weakening. Submitted to Phys Chem Min

Langer K, Flörke OW (1974) Near infrared absorption spectra (4,000–9,000 cm^{-1}) of opals and the role of "water" in these $SiO_2 \cdot nH_2O$ minerals. Fortschr Mineral 52:17–51

Laudise RA (1959) Kinetics of hydrothermal quartz crystallization. J Am Chem Soc 81:562–566

Laudise RA (1973) Hydrothermal growth. In: Crystal Growth, an Introduction. Hartman P (ed) North Holland, Amsterdam, pp 162–197

McLaren AC, Cook RF, Hyde ST, Tobin RC (1983) The mechanisms of the formation and growth of water bubbles and associated dislocation loops in synthetic quartz. Phys Chem Min 9:79–94

Nuttall THD, Weil JA (1980) Two hydrogenic trapped-hole species in α-quartz. Solid State Commun 33, 99–102

Scholze H (1960) Zur Frage der Unterscheidung zwischen H_2O-Molekülen und OH-Gruppen in Gläsern und Mineralien Naturwissenschaften 47:226–227

Stolper EM (1982) Water in silicate glasses: an infrared spectroscopic study. Contrib Mineral Petrol 81:1–17

Stone JG, Walrafren GE (1982) Overtone vibrations of OH groups in fused silica optical fibers. J Chem Phys 76:1712–1727

Van Thiel M, Becker ED, Pimental GC (1957) Infrared studies of hydrogen bonding of water by the matrix isolation technique. J Chem Phys 27:486–490

Received September 30, 1983